(Received 8 September 2025, Accepted 22 October 2025, Scheduled 1 November 2025)

Joint Optimization-Based Beampattern Synthesis for Elliptical-Arc Conformal Frequency Diverse Array

Wei Xu[1,2], Juncheng Ma[1,2,*], Pingping Huang[1,2], Weixian Tan[1,2], and Zhiqi Gao[1,2]

[1] *College of Information Engineering, Inner Mongolia University of Technology, Hohhot 010051, China*
[2] *Inner Mongolia Key Laboratory of Radar Technology and Application, Hohhot 010051, China*

ABSTRACT: To address the engineering challenges of conformal frequency diverse array (FDA) on complex curved surfaces and beamforming optimization, and leveraging the fact that the surface of a streamlined platform can be approximated by an elliptical arc, an elliptical-arc conformal FDA is taken as a representative example, and a conformal frequency diverse array method based on joint parameter optimization (JO-CFDA) is proposed. First, a polygonal approximation model is employed to achieve conformity between the array and the curved surface; then, the parameter α is introduced to control the nonuniform distribution of inter-element spacing along each edge; finally, the parameter β is used to allocate the frequency-offset exponent in a slope-normalized manner. These two parameters work in concert to jointly optimize beam characteristics in both the spatial layout and frequency-domain distribution. Simulation results demonstrate that the proposed method can significantly reduce sidelobe levels and enhance beam directivity while maintaining mainlobe width and peak gain, thereby validating its effectiveness and superiority.

1. INTRODUCTION

Frequency Diverse Array (FDA) radar, first introduced by researchers Antonik et al. from the U.S. Air Force Research Laboratory in 2006 [1], represents a novel radar paradigm. The most important difference of an FDA from a phased-array is that a small amount of frequency increment compared to the carrier frequency is used across the array elements instead of a linear phase shift [2]. In recent years, FDA radars have leveraged their unique range-angle coupling characteristics to demonstrate significant advantages in scenarios such as target detection, interference suppression, and clutter mitigation. Unlike conventional phased arrays that form beams only in the angular domain, FDAs are capable of achieving more flexible energy distribution and focusing in the joint range-angle domain, thereby enhancing anti-jamming capability and target resolution in complex electromagnetic environments. When the frequency offset of the FDA is zero, the FDA is equivalent to a phased array [3]. However, conventional FDA antennas typically employ linear array configurations that cannot conform to streamlined or similarly curved surfaces, resulting in gaps between the array and the platform, which both degrades radiation efficiency and increases aerodynamic drag. In order to enable the deployment of FDAs on streamlined and other complex curved platforms, the concept of conformal FDAs was proposed and has attracted considerable attention within the research community [4–7]. Especially in streamlined application scenarios such as aircraft noses, missile warheads, and shipborne curved hulls, conformal configurations can simultaneously preserve aerodynamic performance and maintain desirable electromagnetic radiation characteristics, thus possessing significant engineering value.

To address the inherent range-angle-dependent beam characteristics of FDA, researchers have conducted extensive studies, primarily adjusting element amplitude, phase, and frequency allocation to improve beam directivity, gain, and sidelobe suppression. Common approaches include employing window-based amplitude weighting functions such as Hamming and Taylor for amplitude shaping, adopting nonlinear or adaptive frequency-offset strategies to enhance range-angle focusing, and introducing intelligent optimization techniques such as genetic algorithms, particle swarm optimization, and differential evolution for beam optimization [8–10]. Although existing methods have achieved significant advances in various single-objective optimization scenarios, most schemes still fail to satisfy engineering requirements when geometric conformity and beam optimization must be addressed concurrently, due to complex manufacturing processes, limited array layout flexibility, and insufficient sidelobe suppression performance.

In light of these challenges, a jointly optimized conformal FDA (JO-CFDA) design method is proposed. In the design process, geometric modeling and frequency-offset allocation are organically coupled to achieve a coordinated optimization of structural conformity and beam characteristics. Taking an elliptical-arc structure as a representative example of streamlined platforms, a polygonal approximation of the arc is employed to enable conformal deployment and closed-form phase compensation. On this basis, two joint parameters, α and β, are introduced to control the spatial distribution density of array elements along the arc and the frequency-offset allocation strategy, respectively. This dual-parameter optimization framework not only establishes a compact yet flexible search space,

* Corresponding author: Juncheng Ma (20231100118@imut.edu.cn).

but also effectively guides beam characteristics toward engineering requirements. By jointly controlling spatial nonuniformity and frequency-offset allocation, the proposed JO-CFDA achieves significant improvements in radiation performance, including effective sidelobe-level reduction, enhanced mainlobe gain, and superior beam focusing, while maintaining conformity to streamlined carrier platforms.

The rest of this paper is organized as follows. Section 2 describes the geometric model and joint optimization framework of the proposed JO-CFDA. The phase-compensation strategy and beampattern synthesis methodology are presented in Section 3. Simulation verifications are provided in Section 4. Finally, the conclusion is drawn in Section 5.

2. JO-CFDA GEOMETRIC MODEL AND JOINT OPTIMIZATION FRAMEWORK

2.1. Geometric Model of JO-CFDA

The surface contour of streamlined platforms such as aircraft noses or missile skins can often be accurately approximated by an elliptical arc, as illustrated in Fig. 1. Therefore, this study adopts an elliptical-arc conformal FDA (JO-CFDA) as a representative example. The local bending of the arc is quantified by the radius of curvature $\rho(\phi)$:

$$\rho(\phi) = \frac{\left(a^2 \sin^2 \phi + b^2 \cos^2 \phi\right)^{3/2}}{ab} \tag{1}$$

where a and b denote the semi-major and semi-minor axes of the ellipse, respectively, and ϕ is the eccentric angle. The curvature is $k(\phi) = 1/\rho(\phi)$; hence a smaller $\rho(\phi)$ corresponds to a tighter local bend and a larger $k(\phi)$. Accordingly, in high-curvature regions the segment length can be shortened or the element density increased to reduce the polygonal approximation error and mitigate curvature-induced phase mismatch.

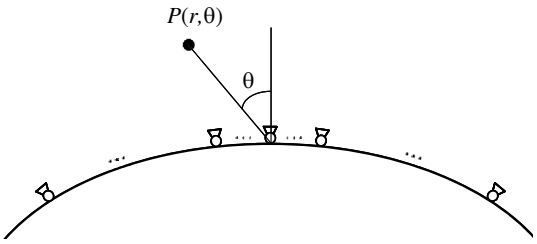

FIGURE 1. Geometric model of the JO-CFDA.

Recognizing the practical difficulty of fabricating a perfectly continuous elliptical arc, the array is modelled as a polygon of $K = 2N + 1$ equal-length linear segments (Fig. 2). To preserve geometric symmetry, the elliptical arc is approximated by a polygonal discretization with an odd number of straight segments.

The resulting JO-CFDA comprises k linear edges: the segment perpendicular to true north is designated as edge 0, and the remaining edges are numbered symmetrically in sequence. Each edge carries $M = 2n + 1$ uniformly spaced elements with inter-element spacing d. By defining the central element

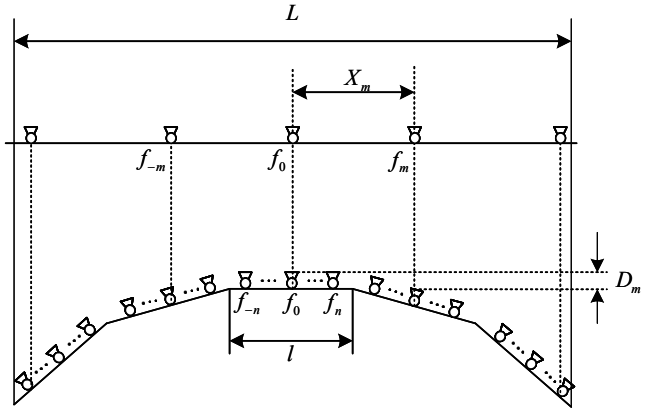

FIGURE 2. Phase compensation of the JO-CFDA.

of edge 0 as the origin and indexing elements symmetrically on either side, the total number of array elements is given by:

$$n_a = K \cdot M \tag{2}$$

,

Although an elliptical arc is used as a representative streamlined contour in this work, the proposed framework does not rely on ellipse-specific geometric properties. After curvature-adaptive piecewise-linear discretization of the target contour, the phase compensation depends only on the local slope and length of each segment. Therefore, the proposed method can be readily generalized to other smooth conformal curves, such as circular arcs as well as parabolic and hyperbolic profiles.

2.2. α-β Beampattern Joint Optimization Framework

Based on the foregoing model, the array elements are uniformly spaced along each linear segment in physical space; however, when being projected onto a constant-phase surface, they undergo a nonlinear mapping jointly governed by the geometry and the incident (look) direction. Consequently, on the constant-phase surface the elements exhibit an edge-dense, center-sparse projected distribution, which elevates the sidelobe level of the FDA and exacerbates range-angle coupling.

To mitigate this effect, two key parameters, α and β, are introduced to jointly optimize the spatial arrangement of elements and the frequency-offset distribution.

First, parameter α is employed to redistribute the inter-element spacing along each edge. For the k-th edge, the element index $m \in \{1, \ldots, M\}$ is normalized into a dimensionless distance measured from the center of that edge:

$$u_m = \frac{|m - g|}{R} \in [0, 1]. \tag{3}$$

where $g = (M + 1)/2$ and $R = (M - 1)/2$. Accordingly, the position parameter of each array element is determined as:

$$t_m(\alpha) = \frac{1}{2} + \frac{1}{2}\mathrm{sgn}(m - g)\, u_m^{\alpha}. \tag{4}$$

where $\mathrm{sgn}(\cdot)$ denotes the sign function. Parameter α provides flexible control over the spatial distribution of element density:

for $\alpha = 1$, the elements are uniformly spaced; for $\alpha > 1$, they concentrate at the midpoint of each edge; and for $0 < \alpha < 1$, they cluster toward the edge endpoints.

As shown in Fig. 3, under $\alpha = 1.5$ the normalized projection spacing of the array elements on the constant-phase surface exhibits pronounced periodic undulations with respect to the element index. The abscissa denotes the element index traversed across successive linear segments, whereas the ordinate represents the projected separation between adjacent elements on the constant-phase surface. Peaks arise near each segment's midpoint (projection stretching), whereas valleys appear near the segment ends (projection compression); consequently, the distribution manifests a nonuniform, edge-dense/center-sparse pattern.

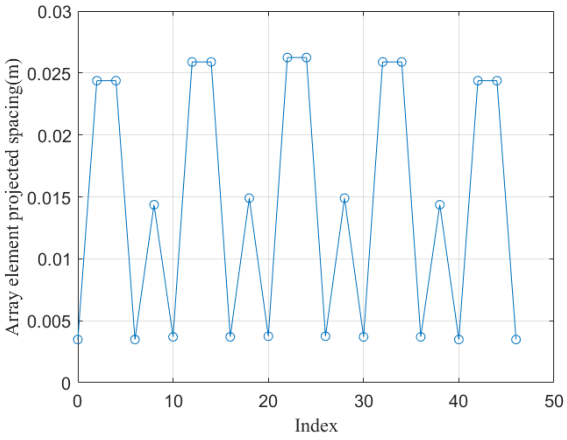

FIGURE 3. Array element projection spacing diagram.

Relative to the uniform case $\alpha = 1$, the setting $\alpha = 1.5$ effectively enlarges the projected spacing in the central region and relieves crowding at the ends, thereby increasing the minimum spacing, reducing the maximum spacing, and yielding more balanced effective sampling. The introduction of the parameter α suppresses sidelobe levels induced by geometric nonuniformity and provides a more stable spatial baseline for the subsequent optimization of frequency-offset allocation.

Based on the spatial distribution determined by α, the parameter β is then introduced to further optimize the allocation of frequency offsets along each edge. Specifically, when the slope of a given edge causes its element projections on the constant-phase surface to become more readily compressed, that edge should be assigned a larger share of the frequency-offset budget so as to suppress sidelobes and mitigate range-angle coupling.

To this end, β is jointly determined by two sources of information: (i) the spatial distribution induced by α, and (ii) the slope of each edge. To guarantee nonnegativity and a unit-sum constraint on the per-edge weights, while smoothly amplifying differences according to the local crowding/sparsity, the frequency offsets are allocated via an exponential normalization scheme:

$$\beta_k = \frac{e^{\alpha m_k}}{\sum_{i=1}^{K} e^{\alpha m_i}} \tag{5}$$

3. JO-CFDA BEAMPATTERN SYNTHESIS

During the beam synthesis procedure of the JO-CFDA, the goal is to ensure that the array generates the desired beam in the specified direction. To achieve optimal beam directivity and sidelobe suppression toward the target, appropriate phase compensation must be applied to each element's signal [11].

3.1. Phase Compensation

According to array-antenna theory, the array factor is defined as the coherent sum of the signals radiated by all elements. To realize beamforming in a specified direction, the signals emitted by each active element must form a constant-phase surface that is perpendicular to the radiation direction. As illustrated in Fig. 2, during the JO-CFDA beam-synthesis process, a phase difference exists between each element and the reference (central) element. To perform scanning on this constant-phase surface, appropriate phase compensation must be applied to the transmitted signals.

As shown in Fig. 2, the projection distance along the vertical axis between the element and the central element can be expressed as:

$$D_m = l \cdot \sum_{i=1}^{N-1} \sin\theta_i + \left(m + (1-2N)n - N + \tfrac{1}{2}\right) \cdot d \sin\theta_N \tag{6}$$

where l represents the length of each linear array element; θ_i is the angle between the normal of the i-th substrate and the due north direction; and the value of i is greater than 1. The distance between the m-th element and the central element, projected onto the vertical axis, can be expressed as:

$$\begin{aligned} X_m \;=\; & \left(\tfrac{1}{2} + \sum_{i=1}^{N-1} \cos\theta_i\right) \cdot l \\ & + \left(m + (1-2N)n - N + \tfrac{1}{2}\right) \cdot d \cos\theta_N \end{aligned} \tag{7}$$

3.2. Beampattern Synthesis

Assuming a carrier frequency of f_c and taking element 0 as the reference element with $f_0 = f_c$, the frequency of the signal transmitted by the m-th element can be expressed as:

$$f_m = f_c + \Delta f_m \tag{8}$$

where Δf_m denotes the frequency offset of the m-th element. Furthermore, Δf_m can be written as:

$$\Delta f_m = \beta \cdot \Delta f_{total} \tag{9}$$

where Δf_{total} represents the total frequency offset.

The transmission signal from the m-th element can be expressed as:

$$X_m(t) = \omega_m \exp\left(j2\pi f_m t\right), \quad 0 < t < T \tag{10}$$

where ω_m represents the complex weight of the m-th element, and T is the duration of the transmitted pulse. The distance from the m-th element to the target point is:

$$r_m = r - X_m \sin\theta \tag{11}$$

The transmitted signal at the expected target point (r_0, θ_0) can be expressed as:

$$X(t,r,\theta) = \sum_{m=-\frac{(n_a-1)}{2}}^{\frac{(n_a-1)}{2}} X_m\left(t-\frac{r_m}{c}\right)$$

$$= \exp\left(j2\pi f_c\left(t-\frac{r}{c}\right)\right) \sum_{m=-\frac{(n_a-1)}{2}}^{\frac{(n_a-1)}{2}} \omega_m$$

$$\times \exp\left(j2\pi\Delta f_m\left(t-\frac{r}{c}\right)\right)\exp\left(j2\pi f_c\frac{X_m\sin\theta}{c}\right) \quad (12)$$

where c is the speed of light.

To control the target at the expected position (r_0, θ_0), the complex weighting vector ω_m can be expressed as:

$$\omega_m = \exp\left(j2\pi\,\Delta f_m\,\frac{r_0}{c}\right) \times \exp\left(-j2\pi f_c\,\frac{X_m\sin\theta_0 + D_m}{c}\right) \quad (13)$$

Therefore, the beam pattern of the expected target can be expressed as:

$$AF(t,r,\theta) = \sum_{m=-\frac{(n_a-1)}{2}}^{\frac{(n_a-1)}{2}} \exp\left(j2\pi\Delta f_m\left(t-\frac{r-r_0}{c}\right)\right)$$

$$\times \exp\left(j2\pi f_c\,\frac{X_m(\sin\theta-\sin\theta_0)-D_m}{c}\right) \quad (14)$$

Accordingly, the beampattern at the target point is given by:

$$B(t,r_0,\theta_0) = \left|\sum_{m=-(n_a-1)/2}^{(n_a-1)/2} \exp\left(\mathrm{j}2\pi\,\Delta f_m\left(t-\frac{r-r_0}{c}\right)\right)\right.$$

$$\left.\times\exp\left(\mathrm{j}2\pi f_c\,\frac{X_m(\sin\theta-\sin\theta_0)-D_m}{c}\right)\right|^2 \quad (15)$$

Although this work focuses on focused beams, the proposed α-β framework is readily applied to shaped-beam synthesis. With α (spatial reparameterization) and β (frequency-offset allocation) fixed, a passband/stopband mask is specified on a discretized (r, θ) grid, and the desired pattern is obtained by optimizing the complex weights $\boldsymbol{\omega}$ so that the passband response approximates the target while the stopband response is kept below a prescribed threshold. The definitions and roles of α and β remain unchanged; the pattern shape is controlled solely via $\boldsymbol{\omega}$. This procedure is consistent with shaped-beam synthesis for fixed-geometry arrays [12].

4. SIMULATION RESULTS

To evaluate the JO-CFDA method's performance in sidelobe suppression and beam characteristics, a squared-law frequency offset was first employed to apply the total frequency offset Δf_{total}. Using the parameters listed in Table 1, α was swept over the interval 0.5–2.5 to investigate its effect on the maximum sidelobe level (SLL). The results indicate that the SLL is minimized at $\alpha = 2$; hence, this value is adopted for all subsequent "α-only optimization" scenarios.

TABLE 1. Simulation parameters

Parameters	Symbol	Value
Carrier frequency	f_c	10 GHz
Frequency offset	Δf	30 kHz
Total number of elements	n_a	105
Number of activated elements	n_{unit}	21
Major axis	a	0.2
Minor axis	b	0.1

Subsequently, three configurations were evaluated: baseline (no α-β joint optimization), α-only optimization ($\alpha = 2$ with uniform β distribution), and full α-β joint optimization. As shown in Fig. 4, the baseline exhibits relatively high sidelobe levels; the α-only optimization, by concentrating elements toward the edge centers, effectively suppresses sidelobes and slightly narrows the mainlobe; and under the full α-β joint optimization, with exponentially normalized frequency-offset assignment, sidelobe suppression is further enhanced, while mainlobe directivity and peak gain are both improved.

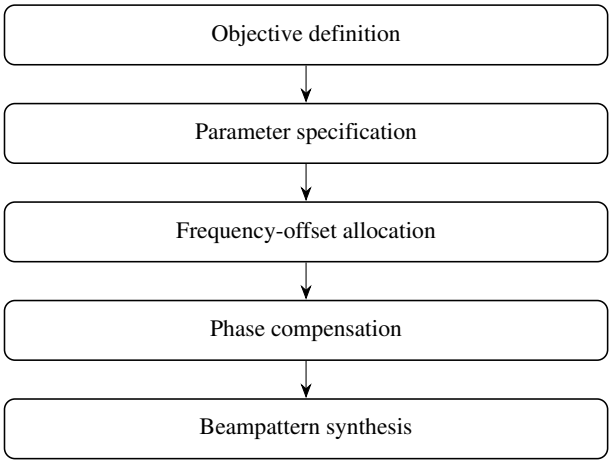

FIGURE 4. Beampattern synthesis flowchart.

All beampatterns in this paper are presented in the power domain as the peak-normalized magnitude of $B = |AF|^2$, so as to enable a direct visual comparison of the joint range-angle energy distribution. For consistency with related work, the corresponding dB representation is obtained as

$$B_{\text{dB}} = 10\log_{10}\left(\frac{B}{\max B}\right) \quad (16)$$

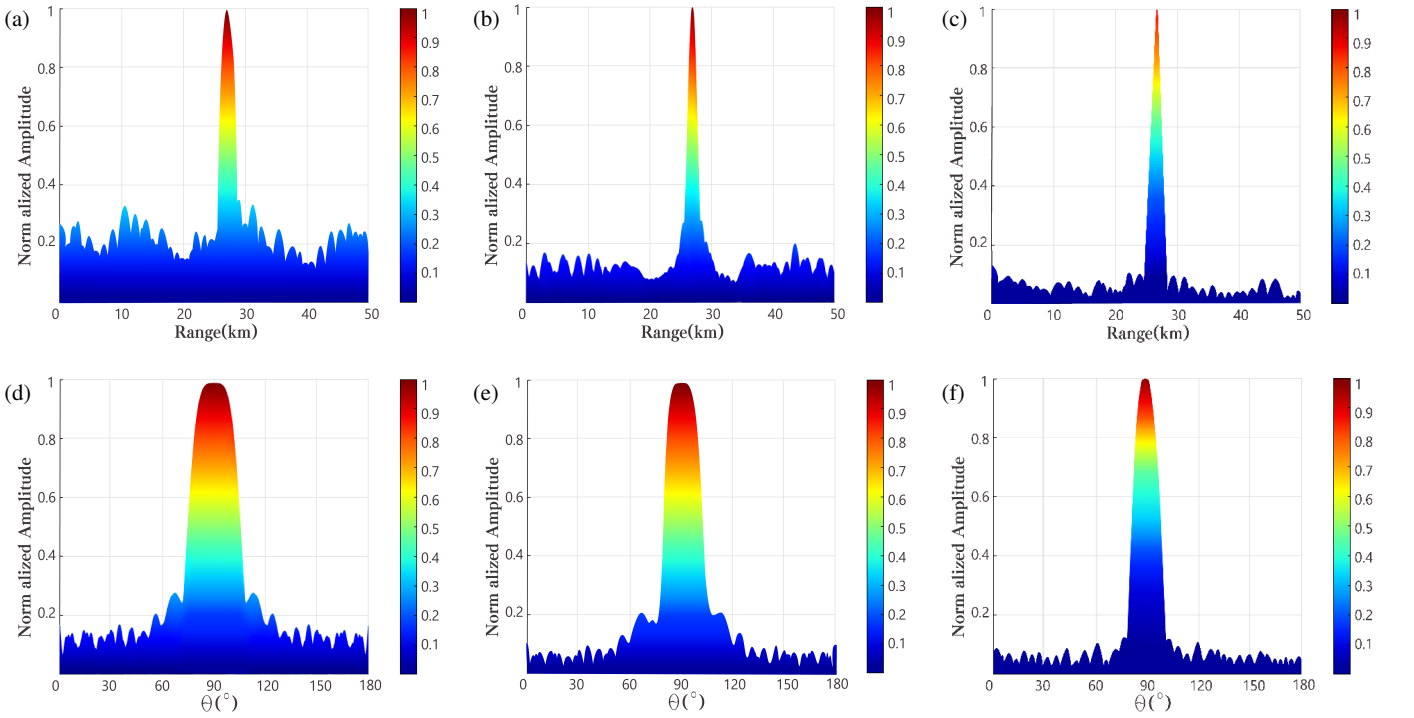

FIGURE 5. Beampattern synthesis results: (a) baseline in the range domain; (b) α-optimized in the range domain; (c) α-β joint optimized in the range domain; (d) baseline in the angle domain; (e) α-optimized in the angle domain; (f) α-β joint optimized in the angle domain.

with 0 dB at the peak. Because dB transform is a monotonic logarithmic mapping of the normalized magnitude, the comparative conclusions in Fig. 5 — namely, sidelobe reduction and mainlobe narrowing — remain unchanged when they are expressed in dB.

On contours with high local curvature, the piecewise-linear (polygonal) approximation incurs larger errors, requiring appropriately denser segmentation (or increased element density) to bound the geometric approximation error; otherwise, sidelobe suppression and beam-focusing performance may degrade. Adaptive segmentation strategies and experimental validation to address this issue will be pursued in future work.

5. CONCLUSION

In this paper, a beam-synthesis method for conformal frequency diverse arrays (JO-CFDAs) based on joint parameter optimization is proposed to address the engineering challenges of conforming FDAs to complex streamlined curved surfaces and optimizing their beam patterns. Taking an elliptical-arc structure as a representative example, the method employs a polygonal approximation to achieve surface conformity and introduces parameters and to optimize, respectively, the spatial distribution of elements and their frequency offsets. Simulation results demonstrate that the joint optimization significantly reduces sidelobe levels and enhances beam directivity while preserving mainlobe performance, thereby demonstrating superior beam-optimization capability and promising practical applicability. The proposed approach thus provides an effective solution for the high-performance beam design of conformal FDAs on streamlined platforms.

ACKNOWLEDGEMENT

This work was supported by the National Natural Science Foundation of China under grant numbers U22A2010.

REFERENCES

[1] Antonik, P., M. C. Wicks, H. D. Griffiths, and C. J. Baker, "Frequency diverse array radars," in *2006 IEEE Conference on Radar*, 3 pp, Verona, NY, USA, 2006.

[2] Wang, W.-Q., "Phased-MIMO radar with frequency diversity for range-dependent beamforming," *IEEE Sensors Journal*, Vol. 13, No. 4, 1320–1328, 2013.

[3] Wang, W., H. Shao, and H. Chen, "Frequency diverse array radar: Concept, principle and application," *Journal of Electronics & Information Technology*, Vol. 38, No. 4, 1000–1011, 2016.

[4] Saeed, S., I. M. Qureshi, W. Khan, and A. Salman, "An investigation into uniform circular frequency diverse array (UCFDA) radars," *Remote Sensing Letters*, Vol. 6, No. 9, 707–714, 2015.

[5] Ding, Z., J. Xie, and L. Yang, "Cognitive conformal subaperturing FDA-MIMO radar for power allocation strategy," *IEEE Transactions on Aerospace and Electronic Systems*, Vol. 59, No. 5, 5072–5083, Oct. 2023.

[6] Tian, X., H. Chen, B. Huang, and W.-Q. Wang, "Fast parameter estimation algorithms for conformal FDA-MIMO radar," *IEEE Sensors Journal*, Vol. 23, No. 24, 30 633–30 641, 2023.

[7] Wang, A., X. Huang, Y. Xu, X. Meng, and Y. Lu, "Thinned and sparse beamforming for semicircular FDAs in the transmit-receive domain," *Remote Sensing*, Vol. 16, No. 17, 3262, Sep. 2024.

[8] Ding, Z., J. Xie, and J. Xu, "A joint array parameters design method based on FDA-MIMO radar," *IEEE Transactions on Aerospace and Electronic Systems*, Vol. 59, No. 3, 2909–2919, Jun. 2023.

[9] Xiao, M., T. Hu, X. Shao, Y. Wu, and Z. Xiao, "An efficient FDA beampattern synthesis method based on SCO technology," *IEEE Antennas and Wireless Propagation Letters*, Vol. 23, No. 10, 3247–3251, Oct. 2024.

[10] Liu, M., C. Wang, J. Gong, M. Tan, L. Bao, and C. Zhou, "Analysis of cantor multistage frequency offset FDA-MIMO beampattern performance," *IEEE Sensors Journal*, Vol. 23, No. 19, 23 270–23 281, Oct. 2023.

[11] Xu, W., C. Pei, P. Huang, W. Tan, and Z. Gao, "Beampattern synthesis and optimization method based on circular frequency diverse array engineering model," *Electronics*, Vol. 13, No. 9, 1618, 2024.

[12] Battaglia, G. M., G. G. Bellizzi, A. F. Morabito, G. Sorbello, and T. Isernia, "A general effective approach to the synthesis of shaped beams for arbitrary fixed-geometry arrays," *Journal of Electromagnetic Waves and Applications*, Vol. 33, No. 18, 2404–2422, 2019.